A Numerical Study on 2D Photonic Crystal Devices for Millimeter and Terahertz Wave Applications

T. Kato[1], **K. Kamata**[1], **C. P. Chen**[1], **T. Anada**[1], **Steve Greedy**[2], **and Trevor Benson**[2]

[1]Kanagawa University, 221-8686, Japan
[2]University of Nottingham, NG7 2RD, UK

Abstract— Novel terahertz functional devices based on photonic crystals are proposed in this paper. The photonic crystal band gap of metal/dielectric rods in an air background is computed using the plane wave expansion method. For metallic rods in air, the frequency dependent dielectric function is described by the Drude model. By adjusting the positions and radii of the metallic and dielectric rods, and their alignment with the lattice, a compact PhC bandpass filter, and T-junction switching circuits are demonstrated.

1. INTRODUCTION

As the demand for greater bandwidth increases alongside the development of the next and future generations of wireless communication systems, the extension of the operating frequency of these systems into the upper-millimeter wave or terahertz region (100 GHz–3 THz) of the electromagnetic spectrum is inevitable [1]. Standardization and regulation activities for THz communications began in 2008 when the IEEE 802.15 Terahertz Interest Group was established to explore wireless systems operating at 300 GHz and beyond [1]. Therefore technologies that enable electronic devices to work in the terahertz region are required, technologies that perform the operations provided by traditional passive circuits; switches, splitters and filters for example. One technology that has shown promise for the realization of such devices is that of silicon (Si) based photonic crystals (PhC) [2].

To date many studies have considered point defect resonators and line defect waveguides in dielectric photonic band gap (PBG) crystals. However, there have been very few studies concerning guided modes in metallic PBG crystals [3]. Nevertheless, it has been suggested that periodic metallic structures have important applications. Recently, planar substrate integrated waveguides (SIW) using metallic via holes have been developed. However, as THz waveguides demand lower loss and higher levels of device integration, some drawbacks become apparent. Recent developments in nanofabrication allow the fabrication of nano-scale 2D arrays of silicon pillars, or holes, resulting in materials with a periodic refractive index that may be utilized as a basis for PhCs. These 2D PhCs can provide a bandgap in every direction of propagation in the lattice's plane of periodicity [3]. In this work, we propose new and compact electromagnetic circuits by embedding the photonic crystal structure into current SIW and non-radiative dielectric (NRD) structures. Through the introduction of point or line defects in the PhCs, the electromagnetic (EM) wave can be controlled, i.e., confined, guided, or localized. Such photonic band gap structures also provide a promising tool for controlling the signal-flow within integrated EM circuits.

In order to design a metallic/dielectric photonic crystal line defect waveguide and point defect high-Q microcavity, the dispersion relations of photonic bandgap are initially calculated using the plane wave expansion method [4]. The frequency characteristics of THz functional devices using photonic crystal line defect waveguides and point-defect resonators are then numerically studied by the finite difference time domain (FDTD) method.

2. 2D METALLIC/DIELECTRIC PHOTONIC CRYSTAL STRUCTURES AND BANDGAP

We consider 2D metallic PhCs consisting of metallic/dielectric rod arrays in air; the PhCs have a square lattice and are embedded inside a parallel-plate metal waveguide, as shown in Figure 1. Compared with dielectric photonic crystals, metallic photonic crystals have the following promising characteristics:

1) Structures composed of metallic photonic crystals may have more compact sizes than those of dielectric PhCs. Since metals are more reflective than dielectrics at few terahertz frequencies, less photonic crystal columns are required to establish band gaps.

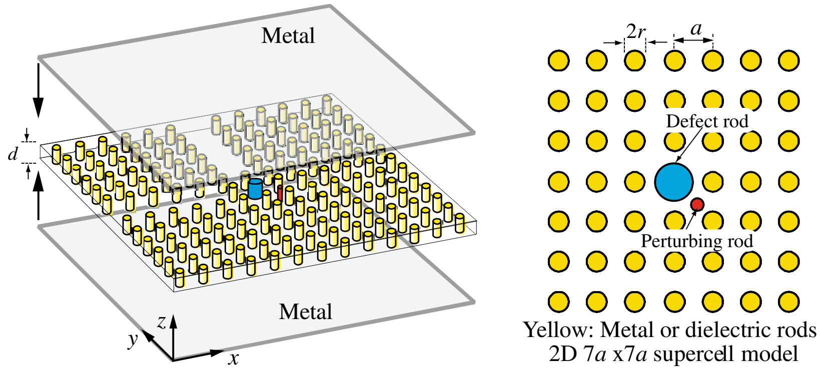

Figure 1: Typical 2D metallic/dielectric photonic crystal model in parallel plate waveguide. R_d is dielectric defect rod (blue) and r_p is perturbing dielectric rod (red).

2) Metallic photonic crystals may enlarge the band gaps, which leaves more margins to the applications. Especially, metallic PhCs operating with E-polarization have a global bandgap that covers the frequency range from zero to cut-off frequency.

The band structure depends on the PhCs geometric and constitutive parameters such as the lattice radius r, lattice constant a and the frequency dependent dielectric constant $\varepsilon(\omega)$. In order to introduce a frequency dependent dielectric function for the metal, time-dependent Maxwell's equations can be written in the following form,

$$\frac{\partial \mathbf{H}}{\partial t} = -\frac{1}{\mu(r)}\nabla \times \mathbf{E} \qquad \frac{\partial \mathbf{E}}{\partial t} = -\frac{1}{\varepsilon(r)}\nabla \times \mathbf{H} - \frac{\sigma(r)}{\varepsilon(r)}\mathbf{E} \tag{1}$$

where $\varepsilon(r)$, $\mu(r)$, and $\sigma(r)$ in above Equation (1) are the position dependent permittivity, permeability, and conductivity of the material, respectively. In the case of M-PhC, we use the frequency dependent Drude model to describe the dielectric constant of metal as follows:

$$\varepsilon_r(\omega) = \left(\varepsilon_\infty - i\frac{\sigma}{\omega\varepsilon_0}\right) = \left(\varepsilon_\infty - \frac{\omega_p^2}{\omega_\tau^2 + \omega^2}\right) + j\frac{\omega_p^2\omega_\tau}{\omega\omega_\tau^2 + \omega^3}, \quad \omega_p = \sqrt{\frac{Ne^2}{m_e}} \quad \text{(Plasma frequency)} \tag{2}$$

where N is the electron density, e is the electron charge, m_e is electron mass, $\omega_\tau/2\pi$ is the damping frequency, and $\omega_p/2\pi$ is the plasma frequency. ε_∞ is the permittivity at infinite frequency. The Drude model parameters used in the calculations for the metal (copper) are $\omega_p/2\pi = 1914\,\text{THz}$ and $\omega_\tau/2\pi = 8.34\,\text{THz}$ [3].

The damping frequency is neglected because it is small compared to the plasma frequency. Thus a simple Drude model is obtained in which the imaginary part of (2) is neglected. Figure 2 shows the computed values of the band gaps obtained by using the standard plane wave expansion (PWE) method. The metallic photonic crystal in Figure 2(a) has a global band-gap for the E polarized field, in the frequency range of a/λ $(= \omega a/2\pi c)$ from 0 to 0.528 (a/λ), the height of metal rods is $d = 0.5a$ and the ratio of the rod's radius to the lattice is $r/a = 0.2$, respectively. While TE modes

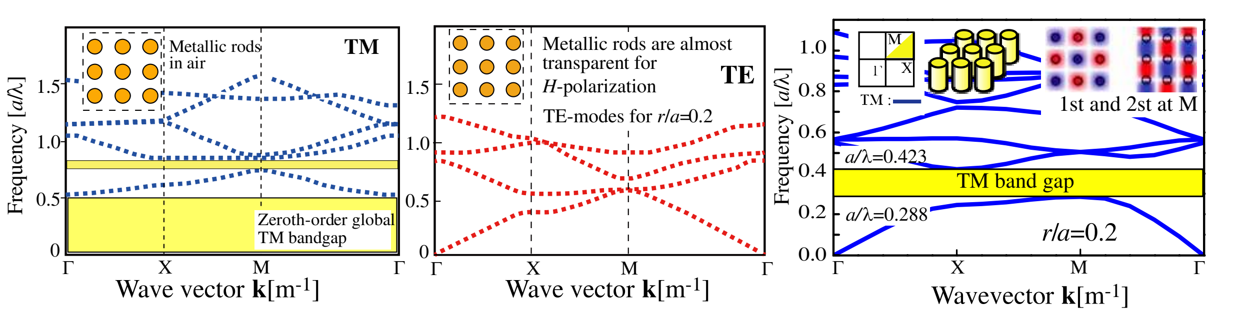

(a) Metal square lattice in air (r/a=0.2) (b) Dielectric square lattice in air (r/a=0.2)

Figure 2: Typical photonic band gap diagrams for metallic and dielectric models.

do not have a cutoff frequency as shown in Figure 2(a). Moreover, a typical dielectric PhC has an index of refraction of $n = 3.40$, which corresponds to high-resistivity and high-purity silicon which is transparent at THz frequencies. Figure 2(b) shows the D-PhC band gap for TM mode obtained by using the standard plane wave method.

3. SIMULATION RESULTS

The validity of our approach is justified through application to examples of a PBG straight waveguides, right angled bend for metallic band-gap waveguides, T-junction power splitter circuits, and PhC narrowband bandpass filters using the double degenerate modes of microcavities.

3.1. Propagation Properties of a Line Defect Straight and Right Angled Bend Waveguide

A PhC right-angled waveguide bend formed within a 2D square lattice of metallic cylinders is considered. Its ability to confine and guide a THz wave, polarized parallel to the PhC rod-axis, i.e., the transverse magnetic (TM) mode, is examined and its performance assessed by considering its transmission characteristics. Propagation loss is a key factor in designing a PhC based waveguide and it is related to the confinement of the guided mode. Figure 3(a) shows the propagation constant of dominant guided mode in metallic PhC line defect waveguide with a conventional metal waveguide of width $W = 1.82a$. They are in a good agreement except upper high frequency region. Figure 3(b) and Figure 3(c) show the frequency response and electric field distributions of a PhC right-angled bend with perfect conductor and Drude models of the metal (copper) conductors. Metallic loss is taken into account with a frequency dependent dielectric constant achieved by the Drude model. Here, the radius of rods and the lattice constant are $r = 11.7\,\mu\text{m}$ and $a = 58.5\,\mu\text{m}$, respectively. From the electric field distributions at increasing frequencies it is observed that the dominant mode couples into the higher-order mode and the bending loss increases rapidly as the range of the confinement, determined by the PBG, is exceeded, and the electromagnetic field is radiated away from the line defect waveguide.

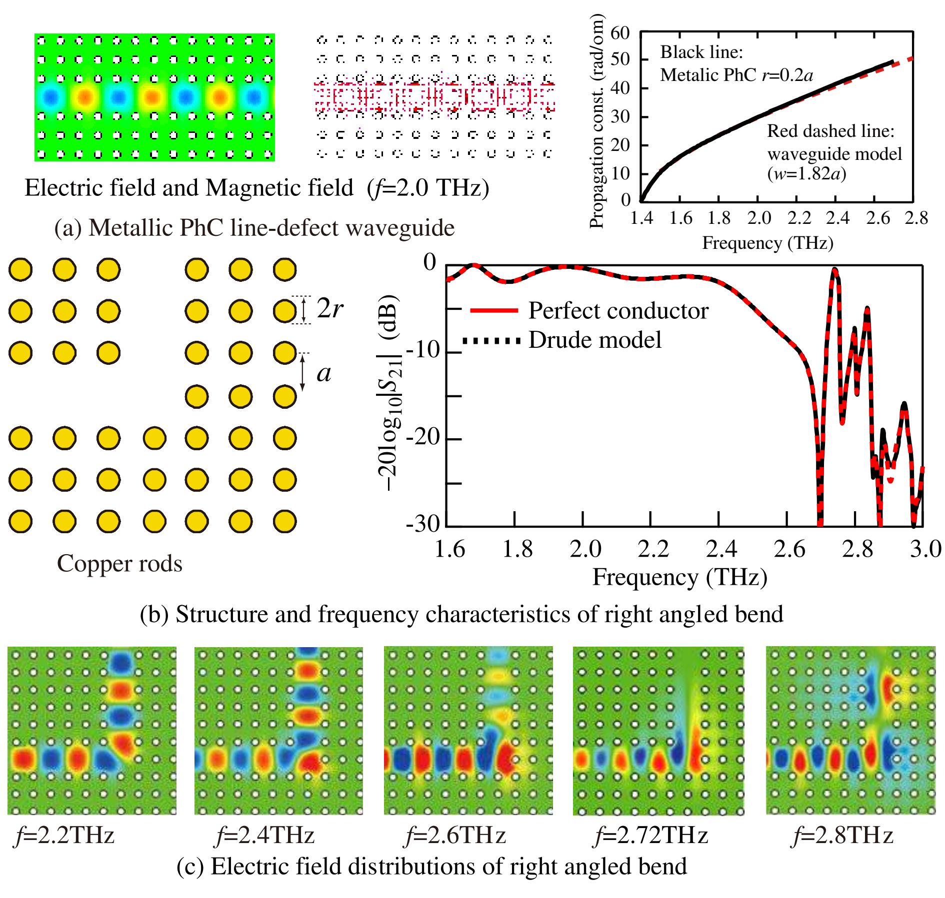

Figure 3: Structure, frequency characteristics and electric field distributions of right angled bend.

3.2. A Metallic Photonic Crystal Switch Created by Inserting a Small Dielectric Perturbing Rod within a T-shaped Waveguide Branches

A novel T-shaped PhC switch is proposed here that can control the direction of an EM-wave that propagates along a line defect waveguide. As shown in Figure 4, the selectivity of the direction is determined by the insertion of a small dielectric rod. The two positions considered for the dielectric perturbing rod (r_p) in the T-junction are $(dx, dy) = (0.0, 0.6a)$ and $(dx, dy) = (-0.65a, 0.65a)$.

(a) When a single rod is placed at $(x, y) = (-0.65a, +0.65a)$, the power, at a frequency $f = 2.15$ THz, fed into port 1 is coupled only to port 3.

(b) When a single rod is placed at $(x, y) = (0, 0.6a)$, at an operating frequency $f = 2.25$ THz, a TM wave incident at port 2 is coupled only to port 3.

(c) When two rods are introduced, Figure 4(c), power at a frequency of $f = 2.10$ THz fed into port 3 couples to only port 4. As shown in Figures 4(c), (d), more complicated network configurations such as interconnects that may contain many branches can be achieved by combining the situations described by (a) and (b) above. The power transmission efficiency is seen to be near 95% at frequency $f = 2.10$ THz. Figures 4(c) and (d) show the almost same frequency response.

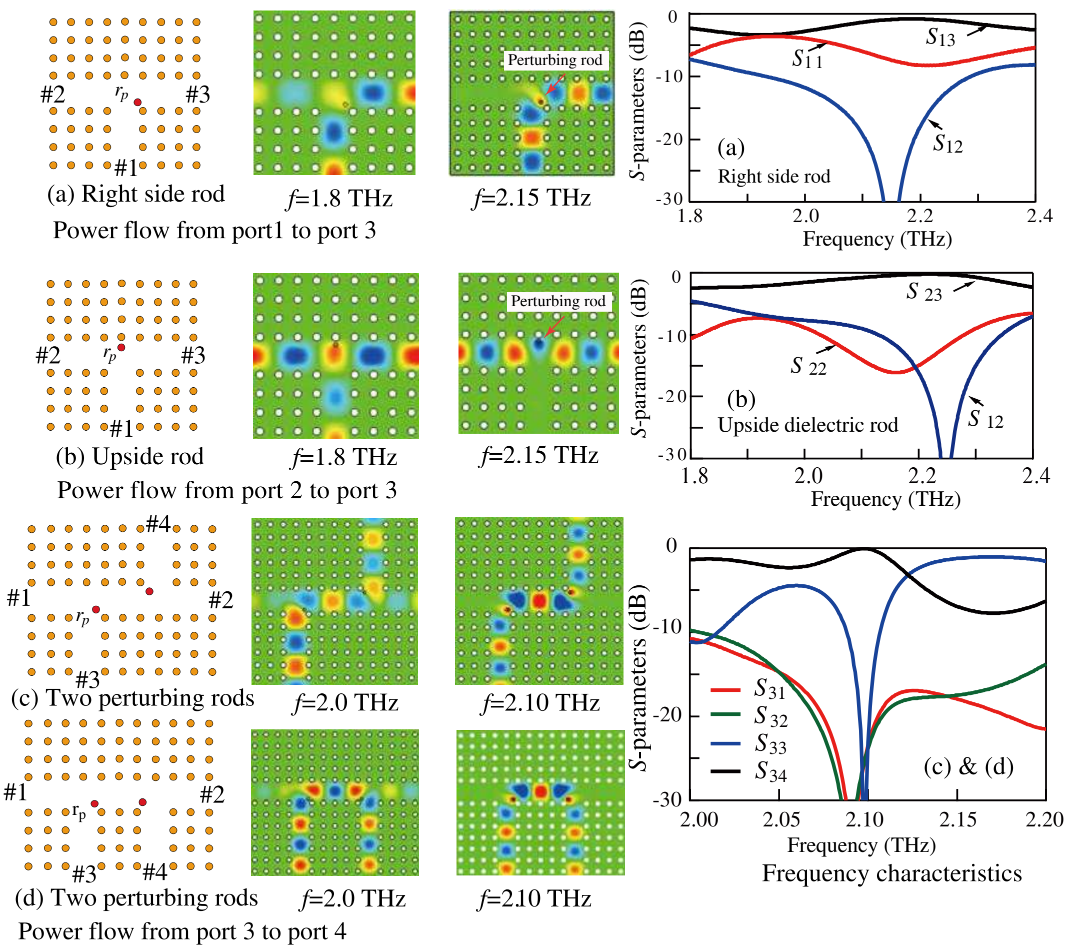

Figure 4: Metallic photonic crystal T-junction power splitter with perturbing dielectric rod. Yellow: metallic PhC and red: dielectric perturbing rod ($r_p = 0.55r$).

As was expected, the EM waves give rise to a **"pull-in" phenomenon** with a small dielectric perturbation rod resulting in a switching function. The PhC switch function is realized by changing the index of the PhC by MEMS, changing the conductance of the semiconductor in the PhC structure, etc..

3.3. A Novel Inductive Window-type Bandpass Filter Using PhC Degenerate Modes

We consider PhC bandpass filter with an additional large dielectric rod of radius R_d and a small dielectric-perturbing rod of radius r_p as shown in Figure 5. By laying out the input/output ports orthogonally (90°), both of the degenerate modes are excited and coupled to each other due to the small perturbing rod within the point defect microcavity. When a small perturbing dielectric rod

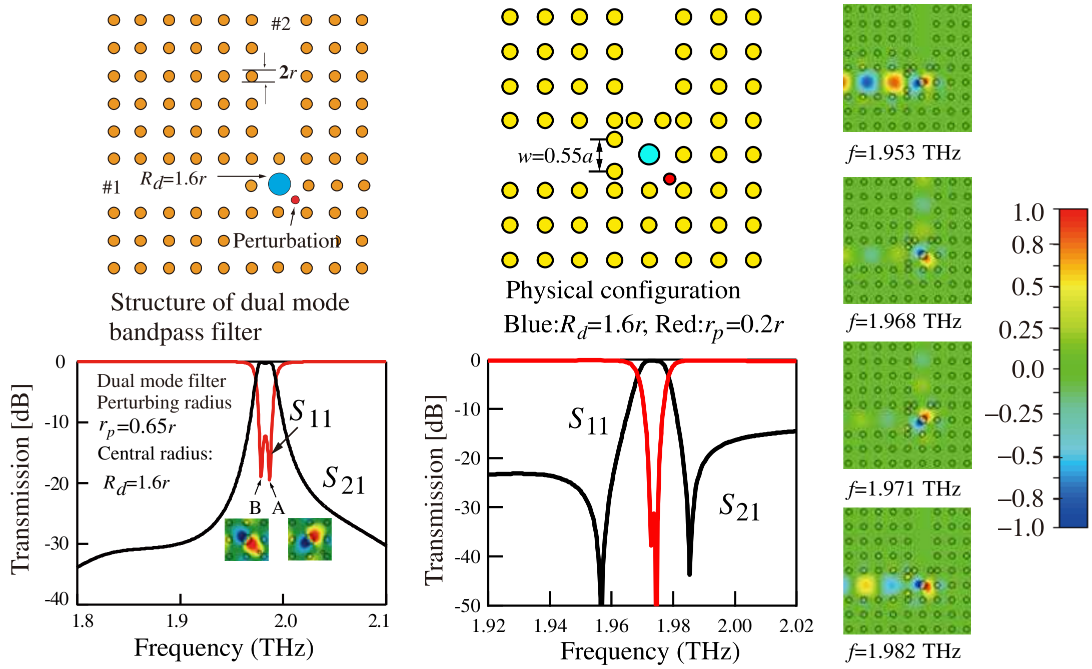

(a) Structure of dual mode bandpass filter

(b) Structure of Pseudo-eliptic function bandpass filter, frequency characteristics, and *Ez* field distributions.

Figure 5: Structure and its properties of proposed photonic crystal bandpass filter.

is added to the dual-mode cavity, as shown in Figure 5(a), the field and resonant frequency will be the sum (= "TM_{210} + TM_{120}") and difference (= "TM_{210} − TM_{120}") of the modes as shown here. By utilizing input-output coupling windows as shown in Figure 5(b), two transmission zeros are created to improve the performance of the filter. Furthermore, two transmission zeros can be simultaneously placed below or above the passband. The input/output coupling structure is inductive with an optimum gap of about $0.5r$. Simulation results show that the resulting bandpass filter exhibits a quasi-elliptic response with two transmission zeros at finite frequencies near the passband as depicted in Figure 5. The filter shows a very good response with a return loss of about 25 dB and a fractional bandwidth of about 5% at a frequency of 1.97 THz. Two identical dual-mode cavity resonators are coupled through inter-coupling rods to achieve the desired frequency response with high selectivity as well as a high-level of compactness.

4. CONCLUSION

The applicability of metallic PhC planar circuits to control signal-flow has been demonstrated in the THz regime. A process of design and simulation has shown that the PhC T-junction type switch can control the direction of propagation of THz waves with specified frequencies. We have also designed bandpass filters consisting of point defect resonators with additional dielectric rods. From these results, we can conclude that the photonic crystal planar circuit shows promise as a key technology for constructing high density integrated electromagnetic circuits. In the near future, the PhC devices proposed here will be applied to EM wave propagations in practical photonic crystal circuits.

REFERENCES

1. Siegel, P. H., "Terahertz technology," *IEEE Trans. Microwave Theory Tech.*, Vol. 50, 910–928, 2002.
2. Johnson, S. G., "MIT applied mathematics photonic crystals: A crash course in designer electromagnetism," http://ab-initio.mit.edu/photons/tutorial/spie-course-2012.pdf.
3. Sigalas, M. M., C. T. Chan, K. M. Ho, and C. M. Soukoulis, "Metallic photonic band gap materials," *Phys. Rev. B*, Vol. 52, 11744–11751, 1995.
4. Kuzmiak, V., A. Maradudin, and F. Pincemin, "Photonic band structures of two-dimensional systems containing metallic components," *Phys. Rev. B*, Vol. 50, 16835–16844, 1994.
5. Fan, S., P. R. Villeneuve, J. D. Joannopoulos, and H. A. Haus, "Channel drop tunneling through localized states," *Physical Review Letters*, Vol. 80, No. 5, 950–963, 1998.